Journal of Applied Polymer Science

Molecularly imprinted polymers for the selective recognition of L-phenylalanine based on 1-buty-3-methylimidazolium ionic liquid

Longfei Yang, Xiaoling Hu, Ping Guan, Ji Li, Danfeng Wu, Bo Gao
Key Laboratory of Space Applied Physics and Chemistry, School of Natural and Applied Science, Northwestern Polytechnical University, Xi'an 710072, China
Correspondence to: L. Yang (E-mail: yanglf86@163.com)

ABSTRACT: To enhance the affinity of 4-vinyl pyridine to L-phenylalanine (L-Phe) and convert the imprinting process from the aqueous phase to the organic phase, an oil-soluble amino acid ionic liquid was introduced as a template. In this study, 1-butyl-3-methylimidazolium α-aminohydrocinnamic acid salt was first applied to prepared surface molecularly imprinted polymers (MIPs) in acetonitrile for the selective recognition of L-Phe. Fluorescence quenching analysis of the functional monomer on the template was investigated under different conditions to study the imprinting mechanism. Several binding studies, such as the sorption kinetics, sorption thermodynamics, and solid-phase extraction application, and the chiral resolution of racemic phenylalanine were investigated. The binding isotherms were fitted by nonlinear regression to the Freundlich model to investigate the recognition mechanism. The affinity distribution analysis revealed that polymers imprinted by ionic liquid showed higher homogeneous binding sites than those imprinted by L-Phe. The competition tests were conducted by a molecularly imprinting solid-phase extraction procedure to estimate the selective separation properties of the MIPs for L-Phe. The target MIP was shown to be successfully for the separation of L-Phe from an amino acid mixture. © 2015 Wiley Periodicals, Inc. J. Appl. Polym. Sci. **2015**, *132*, 42485.

KEYWORDS: adsorption; functionalization of polymers; ionic liquids; kinetics; molecular recognition

Received 3 December 2014; accepted 10 May 2015
DOI: 10.1002/app.42485

INTRODUCTION

L-Phenylalanine (L-Phe) is one of eight essential amino acids that the body cannot synthesize itself. It is used commonly as a food additive and in pharmaceuticals in infusion fluids or for the chemical synthesis of pharmaceutically active compounds.[1] A recent report of the separation and analysis of L-Phe mainly based on high-performance liquid chromatography,[2] membrane separation,[3] and electrochemical sensors.[4] However, these methods have their drawbacks, such as a relatively low separation selectivity, expensive chiral column, and complicated preparation process; this restricts its application in the separation of chiral amino acids and amino acid mixture. Therefore, to overcome these shortcomings, it is necessary to establish a rapid, low-cost, and efficient method for separating L-Phe specifically or for the resolution of racemic phenylalanine. Molecular imprinting technology, which is mainly based on the formation of noncovalent or covalent interactions[5] between a monomer and template, has been extensively used in the area of electrochemical sensors,[6] pretreatment of samples,[7] and product enrichment and separation.[8] The interaction between the common imprinting process is mainly based on hydrogen bonding; this is usually disrupted in polar solvents. Molecularly imprinted polymers (MIPs) prepared in this process show a low selectivity of L-Phe; this might be due to the simple hydrogen-bonding interactions between each monomer and L-Phe. Hydrogen bonding is more susceptible to polar solvents or protic solvents than electrostatic forces and π–π stacking interactions.[9–11] Studies have revealed that the existence of strong polar and proton solvents, especially for water, will cause severe damage to hydrogen-bonding interactions and will eventually affect the recognition properties of MIPs.[5] Even worse, most amino acids, peptides, and proteins are water soluble; as a result, the imprinting process has to be completed in the presence of water. The complex solvent environment[12] and weak interactions contribute to the low proportion of template–monomer complexes, and this leads to binding site heterogeneity. Binding site heterogeneity, which affects the imprinting efficiency of MIPs, is a fundamental problem of the imprinting process. Therefore, for amino acid imprinting, which is mainly based on hydrogen-bonding interactions, it is necessary to enhance the interactions between the template and the monomer; this will eventually limit the damage on the formation of complexes. Therefore, on the basis of this consideration, there is an urgent need to explore some novel template analogues, which are not

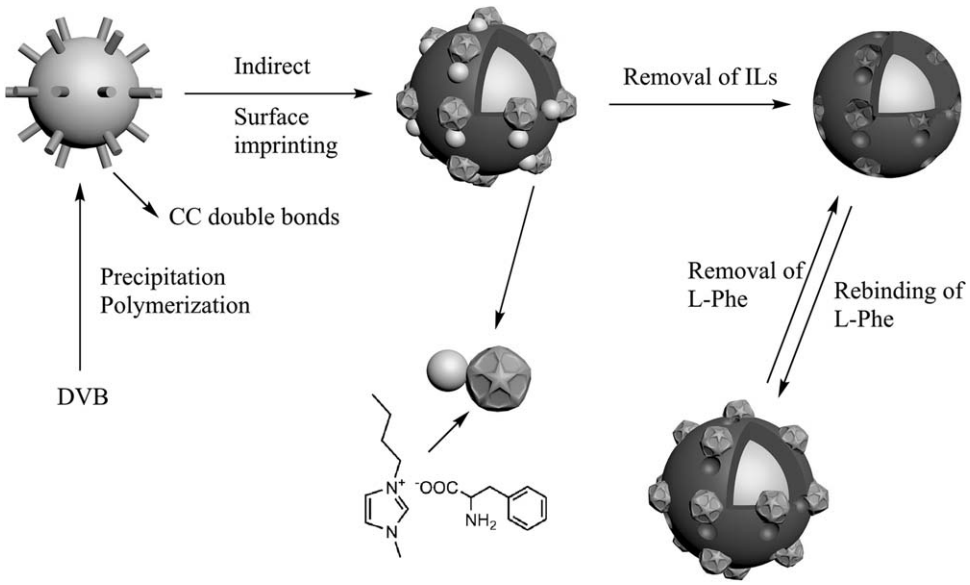

Figure 1. Protocol for the synthesis of MIPs.

only soluble in organic solvents but can also interact with amino acids via multiple interactions in addition to hydrogen-bonding interactions. Therefore, once the hydrogen-bonding interactions are partially damaged by solvent molecules or other solvents, strong interactions can also be formed between functional monomers and amino acids; this will result in a high imprinting efficiency and a good specificity in the separation of amino acids. This is also a trend of biological molecules imprinted in organic media.

The template analogue technique will convert the hydrophilic template imprinting process from water to the organic phase and change the type of self-assembly. Alizadeh and Zeynali[13] introduced an analogue imprinting technique to prepare an electronic nose. The electronic nose was able to recognize the individual components in a binary mixture. Tominaga *et al.*[14] used the prepared polymer imprinted by ionic groups of the template as the selective recognition of paralytic shellfish poison and saxitoxin. The template analogue had relative stable interactions with the monomers and should be soluble in less polar or aprotic solvents. Amino acid ionic liquids (AAILs), typically composed of organic cations and amino acid anions, are soluble in many kinds of organic solvents. AAILs have very good compatibility with many kinds of monomers. Ionic liquids (ILs) are nonvolatile, polar, thermally stable compounds. In recent years, ILs have been used in molecular imprinting science as stabilizers for protein,[15] reaction solvents,[16] and monomers. ILs have relatively strong electrostatic interactions, moderate hydrogen-bonding, and π–π interactions in the template in imprinting process. Researchers[17] have shown that MIPs prepared in 1-butyl-3-methylimidazolium tetrafluoroborate were two times more selective than the corresponding MIPs generated under traditional precipitation conditions. ILs can not only accelerate the synthesis but also improve the selectivity of transaconitic acid imprinted polymers. However, IL in such a procedure make the imprinting process more complicated; this is not conducive to the research of the imprinting mechanism. The use of ILs as template analogues provide perhaps direct access to MIPs with highly selective recognition properties.

Inspired by all of the above, we propose a simple and innovative method for preparing an L-Phe imprinted polymer in an organic solvent. We introduced 1-butyl-3-methylimidazolium α-aminohydrocinnamic acid salt ([BMIM][Phe]) as the template; it has strong electrostatic forces generated by the carboxylate anions, benzene rings, and amino groups. The imprinting mechanism was investigated by fluorescence quenching analysis. Moreover, [BMIM][Phe] provided an effective solution for preparing MIPs with high selectivity and gave a better identifying performance. The recognition ability of the MIPs were conducted in various adsorption tests compared with L-Phe imprinted polymers/nonimprinted polymers (NIPs). The results of molecular recognition mechanism demonstrated that [BMIM][Phe] imprinting process increased the proportion of specific binding sites on the surface of the polymer, realized better specificity and homogeneity, and then caused a higher degree of polymerization. The preparation of the MIPs and the identification and elution processes are shown in Figure 1.

EXPERIMENTAL

Materials and Reagents

1-Butyl-3-methylimidazolium was purchased from Chengjie Chemical Co., Ltd. L-Phe (99.5%), L-histidine (L-His; 99.5%), and L-tryptophan (L-Trp; 99.5%) were obtained from Wako (Japan) and were used as received. Ethylene glycol dimethacrylate (EDMA; 98%), 4-vinyl pyridine (4-vp; 95%), and divinylbenzene (DVB; 95%) were purchased from Sigma–Aldrich (Darmstadt, Germany) and were distilled *in vacuo* to remove the polymerization inhibitor. Azodiisobutyronitrile of analytical grade was purchased from Damao Reagent Plant (Tianjin, China) and was purified by recrystallization from methanol before use.

Fourier transform infrared spectra (4000–400 cm^{-1}) in KBr were recorded with a Vector 22 spectrometer (Bruker,

Table I. Recipes for the Preparation of the Polymers

Sequence	Template (mmol)		Monomer (mmol): 4-vp	Crosslinker: EDMA (mmol)	Solvent (mL)	
	[BMIM][Phe]	L-Phe			Acetonitrile	H^2O
MIP1	0.23	0	1.38	5.40	50.0	0
MIP2	0.23	0	1.38	5.40	30.0	20.0
MIP3	0	0.23	1.38	5.40	30.0	20.0
NIP1	0	0	1.38	5.40	50.0	0
NIP2	0	0	1.38	5.40	30.0	20.0

http://brukeroptics.equips.cn). The scanning electron microscopy images were recorded by a Quanta 600FEG instrument (FEI). The data of the binding experiments were detected by ultraviolet–visible (UV–vis) absorption spectra (U-3900 Hitachi spectrometer). All of the separations were performed on a Shimadzu HPLC system (Shimadzu, Japan) equipped with a Shimadzu SPD-20AVP ultraviolet detector and a Hypersil-ODSC18 column (4.6 × 250.0 mm^2, Thermo). A Chirascan circular dichroism (CD) spectrometer (Applied Photophysics, Ltd., United Kingdom) was used for CD spectrum measurements. Surface property analysis was performed by nitrogen sorption porosimetry on a surface area and porosimetry analyzer (TriStarII 3020).

Synthesis and Characterization of [BMIM][Phe]

1-Butyl-3-methylimidazolium bromide (0.02 mol) was dissolved in 10.0 mL of water. To prepare a 1-butyl-3-methylimidazolium hydroxide aqueous solution, the anion-exchange process was conducted with Amberlite 717. A slight excess of L-Phe (0.024 mol) was added to an aqueous solution of 1-butyl-3-methylimidazolium hydroxide aqueous to prepare [BMIM][Phe]. The reaction mixture was then heated to 40°C for 24 h to complete neutralization. After the solvent and excess L-Phe were removed, the target product, a nearly colorless transparent viscous liquid, was obtained. The structure of [BMIM][Phe] was examined with ^{1}H-NMR to confirm it.

^{1}H-NMR (400 MHz, DMSO-d_6, δ): 0.88 (t, 3H, CH_3), 1.24 (m, 2H, CH_2), 1.75 (m, 2H, CH_2), 2.52 (q, 1H, NH_2—CH), 3.07 (m, 2H, NH_2—CH—CH_2), 3.42 (d, 2H, NH_2), 3.87 (s, 3H, CH_3), 4.18 (t, 2H, $CH_2CH_2CH_2CH_3$), 7.12 (m, 1H, $C_6H_5^1$), 7.21 (t, 4H,$C_6H_5^4$), 7.77 [s, 1H,C(5)H], 7.83 [s, 1H,C(4)H], 9.77 [s, 1H, C(2)H].

Fluorescence Quenching Measurements

The fluorescence intensities were recorded with a PerkinElmer LS5 luminescence phosphorescence spectrophotometer with 5.0-nm excitation and 10.0-nm emission slit widths. The maximum excitation wavelength and maximum emission wavelength for L-Phe and [BMIM][Phe] were 300 and 540 nm, respectively. A value of 50 μ*M* [BMIM][Phe] was chosen as the concentration for fluorescence quenching experiments. A dilution series of 4-vp solutions (1.5–7.5 m*M*) were prepared in acetonitrile. For each data point, 0.25 mL of the appropriate 4-vp solution was added to 3 mL of template solution to give a final flavonoid concentration in the range 50–250 μ*M*. The change in the fluorescence emission intensity was measured after 10 min of the addition of flavonoid to the template. The addition of a constant volume of quencher to the template solution prevented complications due to dilution effects within titration-type experiments. Each measurement was repeated in triplicate, and the means were calculated. For the fluorescence quenching study of 4-vp to [BMIM][Phe] and L-Phe in acetonitrile/H_2O (3:2 v/v), the same procedure as mentioned previously was used.

Preparation of the Polydivinylbenzene Microspheres with Precipitation Polymerization

In a standard recipe, zeolite(2 g) and azobisisobutyronitrile (0.2688 g, 2 wt % relative to DVB) was added to a solution of DVB (12.5 mL, 13.4400 g, 5 vol % relative to the total volume) in acetonitrile (250.0 mL) in a 500.0-mL one-necked flask fitted with a condenser. Then, the mixture was degassed by the bubbling of dried argon for 20 min. After 6 h of reaction in a boiling solution, the deposit was filtered and repeatedly washed by ethanol.

Preparation of the Molecularly Imprinted and Nonimprinted Core–Shell Microspheres

MIP1 was prepared by the copolymerization of 4-vp and EDMA in the presence of [BMIM][Phe] as a template and the polydivinylbenzene as the core. The detailed procedures are as follows: 0.23 [BMIM][Phe] and 1.35 mmol 4-vp were dissolved in 50.0 mL of acetonitrile. The mixed solution, placed in a 100.0-mL flask equipped with a reflux condenser, was stirred at 25°C for 4 h to form a monomer–template complex; this was followed by the addition of 5.40 mmol of EDMA, 0.20 mmol of azobisisobutyronitrile, and 0.30 g of polydivinylbenzene microspheres. The mixture was purged with pure argon for 20 min and left to react at 65°C for 24 h under stirring. The products were centrifuged under 8000 rpm for 10 min. The resulting solid was obtained and washed ultrasonically with ethanol until no monomer and crosslinker could be detected in the washing solution by a UV–vis spectrophotometer. The obtained polymer was further eluted with a sodium chloride solution (1 wt %) until no template could be detected by a UV–vis spectrophotometer and was then eluted with deionized water. The preparation of core–shell MIP2, MIP3, NIP1, and NIP2 was done with the aforementioned procedures except for different templates and solutions. Detailed recipes for the preparation of the polymers are shown in Table I.

Binding Experiments

All adsorption isotherm experiments were carried out in a thermostatic orbital shaker at 100 rpm and 25°C. To evaluate the binding capacities of the [BMIM][Phe] imprinted polymer,

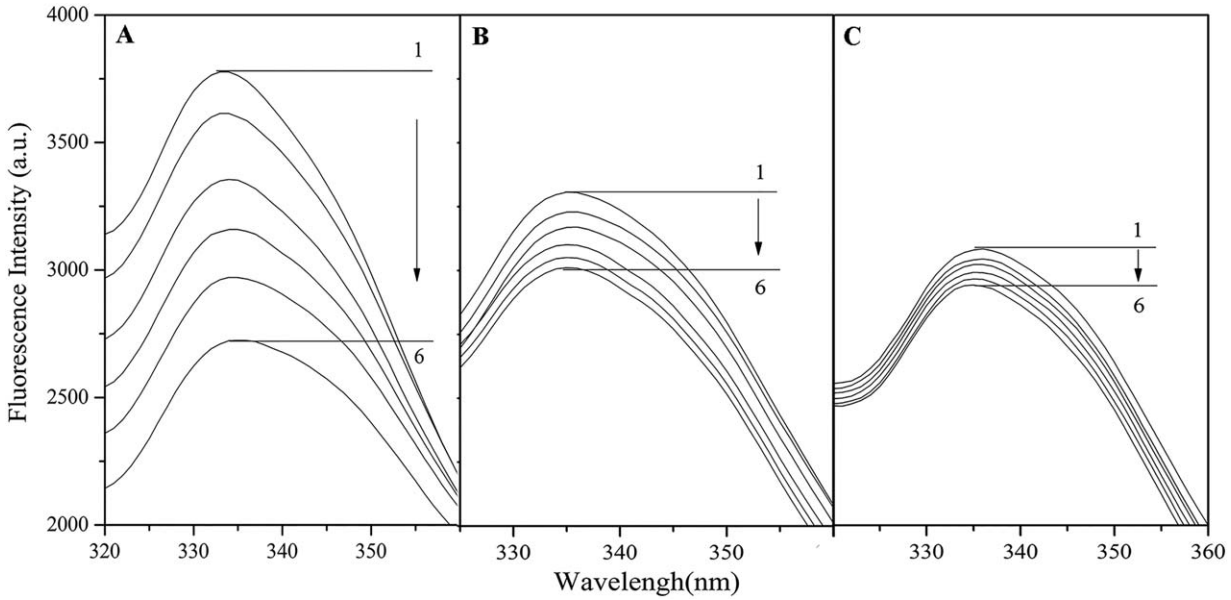

Figure 2. Fluorescence quenching spectra of (A) 50 μM [BMIM][Phe] in acetonitrile, (B) [BMIM][Phe] in acetonitrile/H_2O, and (C) L-Phe in acetonitrile/H_2O. Spectra 1–6 correspond to 4-vp concentrations of 0, 50, 100, 150, 200, and 250 μM.

0.15 g of the polymer was added to 5.0 mL of L-Phe standard water solutions in a 10.0-mL test tube with various concentrations ranging from 0.05 to 1.30 mg/mL. After being shaken for 10 h, the microspheres were removed by centrifugation at 8000 rpm for 10 min, and the supernatant was withdrawn and measured by UV spectrometry at 257.5 nm. The adsorption capacity was calculated according to the following equation:

$$Q=\frac{(C_0-C_e)\times V}{m} \quad (1)$$

where Q is the adsorption capacity of the polymers (mg/g); C_0 and C_e are the initial and final concentrations of the L-Phe in the solution (mg/mL), respectively; V is the cubage of the solution (mL), and m is the mass of the polymer (mg).

To investigate the binding kinetics, batch adsorption experiments were carried out at 25°C and at 100 rpm on an thermostatic orbital shaker, and 0.15 g of polymer was placed in a 15.0-mL test cube containing L-Phe water solutions (1.40 mg/mL). All of the adsorption experiments were conducted in triplicate, and the average value was adopted.

Solid-Phase Extraction and Chiral Resolution Procedures

Molecularly imprinted solid-phase extraction (MISPE) columns were prepared by the packing of the dry MIPs (0.5 g) in a solid-phase extraction cartridge (total volume = 3.0 mL and diameter = 8 mm). One polytetrafluoroethylene filter was placed at the bottom; another was placed at the top of the cartridge. Before the analyte was loaded, the MISPE columns were previously conditioned with 2.0 mL of acetonitrile/H_2O (3 : 2 v/v). To investigate the selective adsorption ability of L-Phe from the mixed solution, the binding abilities of MIP1, MIP2, and MIP3 for L-Phe, L-Trp, and L-His were evaluated. L-Trp and L-His had a similar molecular structure to L-Phe. Solutions containing L-Phe, L-Trp, and L-His were separated by solid-phase extraction. The concentration of the components was 1.0 μmol/mL in acetonitrile/H_2O (3 : 2 v/v), respectively. After 2.0-mL solutions containing different amino acids passed through the columns at a flow rate of 0.20 mL/min, the columns were washed with 2.0 mL of acetonitrile/H_2O (v/v = 9 : 1) at the same flow rate. The analyte retained on the polymers was eluted with 5.0 mL of a H_2O/acetic acid solution (v/v = 9 : 1). The eluent was evaporated to dryness *in vacuo* at 25°C, and the residue was redissolved into 3.0 mL of deionized water for further HPLC analysis.

As to chiral resolution procedures, the MISPE column was previously conditioned with 2.0 mL of acetonitrile/H_2O (3 : 2 v/v), and then, the solution containing racemic phenylalanine (2.0 μmol/mL) were separated by MISPE. The subsequent process was the same as previously mentioned. The eluent was analyzed by CD spectral measurement.

RESULTS AND DISCUSSION

Fluorescence Quenching Analysis of the Imprinting Mechanism

As is known to us, interaction between the template molecule and monomer in the prepolymerization process is a crucial factor in a successful imprinting protocol.[18] Figure 2 shows the fluorescence spectra of [BMIM][Phe] and L-Phe with a series of concentrations of 4-vp in different solvents. There was no apparent maximum emission wavelength shift. This means that the molecular conformation of the [BMIM][Phe] and L-Phe were not affected whatever the 4-vp mechanism of interaction. As shown in Figure 2(A), the fluorescence intensity of [BMIM][Phe] showed a notable decrease when 4-vp was added to [BMIM][Phe] in the acetonitrile solution. As also shown in Figure 2(B), the fluorescence lowering magnitude was smaller in the acetonitrile/H_2O solution than in the acetonitrile solution; this suggests that [BMIM][Phe] bonded 4-vp more strongly in acetonitrile than in acetonitrile/H_2O. As shown in Figure 2(C),

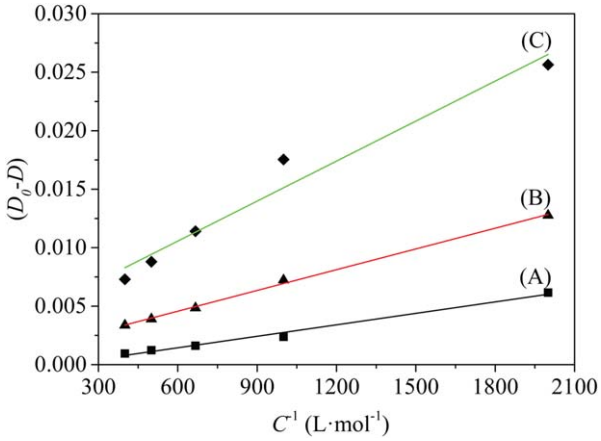

Figure 3. Lineweaver–Burk curve of the fluorescence quenching of (A) [BMIM][Phe] with 4-vp in acetonitrile, (B) [BMIM][Phe] with 4-vp in acetonitrile/H_2O, and (C) L-Phe with 4-vp in acetonitrile/H_2O. [Color figure can be viewed in the online issue, which is available at www.interscience.wiley.com.]

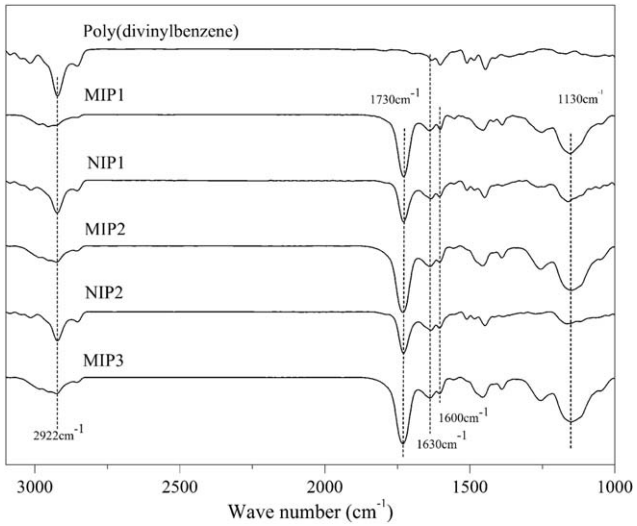

Figure 4. Fourier transform infrared spectra of (A) polydivinylbenzene, (B) MIP1, (C) NIP1, (D) MIP2, (E) NIP2, and (F) MIP3.

the fluorescence intensity of L-Phe showed a weak decrease when 4-vp was added to the acetonitrile solution.

The fluorescence quenching was described by the Lineweaver–Burk equation:[19]

$$\frac{1}{D_0-D}=\frac{1}{D_0K_{LB}C}+D_0 \quad (2)$$

where D_0 and D are the fluorescence intensities before and after the addition of the quencher, respectively; C is the concentration of the quencher; and K_{LB} is the Lineweaver–Burk quenching constant. Hence, eq. (2) was applied to determine K_{LB} by the linear regression of a plot of $(D_0 - D)^{-1}$ against C^{-1}.

The Lineweaver–Burk curves of the quenching of [BMIM][Phe] fluorescence by 4-vp were derived, as shown in Figure 3. Thus, the binding constants were obtained from the slopes of the curves, as listed in Table II.

The results show that the fluorescence of L-Phe and [BMIM][Phe] was quenched through a static quenching procedure by a functional monomer because of the formation of template–monomer complexes. The data showed that the affinity of 4-vp to [BMIM][Phe] in acetonitrile was about three times that of 4-vp to L-Phe. The affinity of 4-vp to [BMIM][Phe] in acetonitrile/H_2O was about two times that of 4-vp to L-Phe. This indicated that [BMIM][Phe] may have been the better template; it had stronger interaction with 4-vp. More importantly, acetonitrile caused less damage to the template–monomer complexes. The previous result further supported our inference that the higher affinity of 4-vp to [BMIM][Phe] in acetonitrile might have been responsible for the molecular recognition performances.

Table II. Lineweaver–Burk Binding Constants

System	Solvent	K_{LB} (L/mol)	R^2
[BMIM][Phe]-4-vp	Acetonitrile	81.05 ± 1.04	0.9850
[BMIM][Phe]-4-vp	Acetonitrile/H_2O	51.12 ± 1.51	0.9974
L-Phe-4-vp	Acetonitrile/H_2O	28.49 ± 1.32	0.9829

IR Spectroscopy and Microstructure of the Core–Shell Polymers

The Fourier transform infrared spectra of the polymers is shown in Figure 4. For the MIP1, NIP1, MIP2, NIP2, MIP3, two novel absorption bands at 1730 and 1130 cm^{-1} were observed; these corresponded to the stretching vibrations of C═O and C—O—C (the characteristic carbonyl peaks introduced by EDMA, respectively). The peak corresponding to the C═N stretching (1600 cm^{-1}) in the pyridine rings was also observed in the spectra; this revealed that poly(4-vinyl pyridine) was present in the MIPs. This result indicated that the shell polymers were successfully introduced onto the surface of the polydivinylbenzene by a copolymerization reaction. The bands at 1630, 1493, and 1452 cm^{-1} was assigned to the characteristic absorption peak of the benzene ring.

The size and surface morphology of the polymers were detected by scanning electron microscopy, as shown in Figure 5. As we observed, the geometrical mean diameter of the original polydivinylbenzene prepared by precipitation polymerization was about 2.5 μm [Figure 5(F)]. Figure 5(A) shows a scanning electron microscopy image of MIP1. The surface was completely covered by the imprinted shell; this indicated that a polymer layer was successfully grafted onto the surface of polydivinylbenzene. In addition, the surface morphology of MIP1 had a greater difference than MIP2 and MIP3, especially MIP3. Under the conditions of different templates in the same solvent, the shell was thicker and rougher because of the introduction of ILs; this significantly improved the conversion percentages of the functional monomer in the polymerization reaction.[20] The conversion percentages of the shell of A, B, C, D, and E were 92, 44, 45, 96, and 55%, respectively. This may have been related to the increasing polarity of the medium favor transition states involving charge transfer and complex formation between

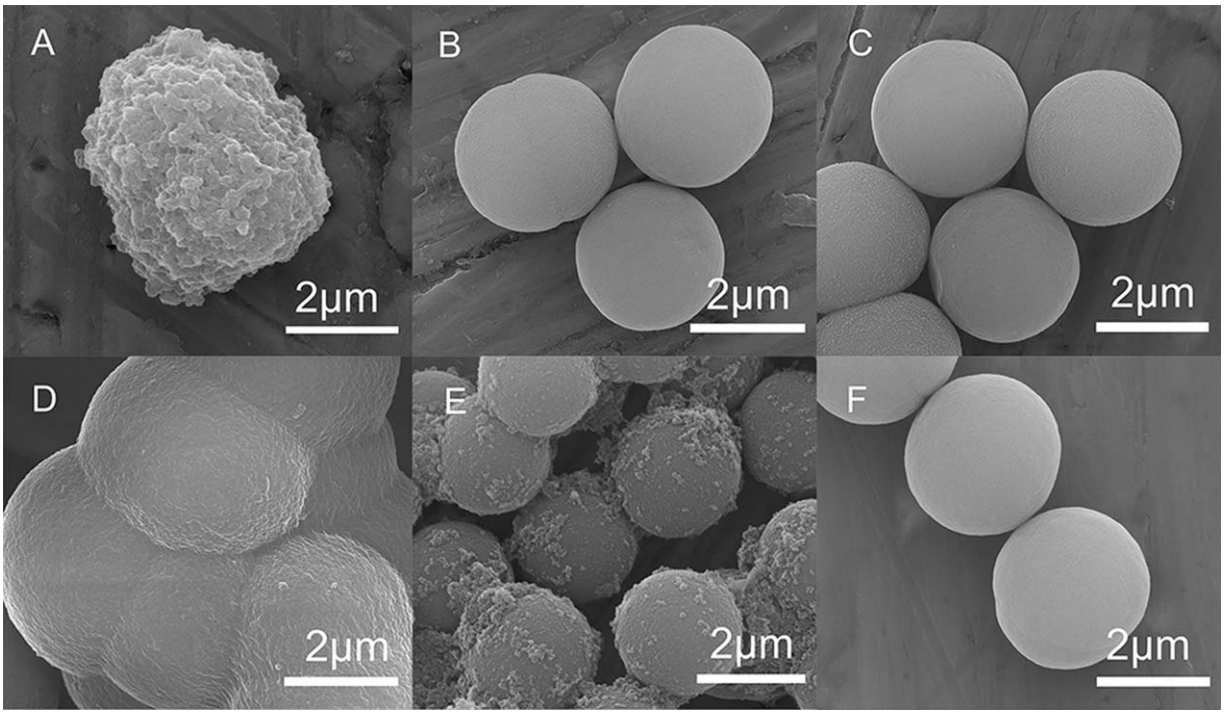

Figure 5. Surface morphology of (A) MIP1, (B) MIP3, (C) NIP1, (D) MIP2, (E) NIP2, and (F) polydivinylbenzene.

[BMIM][Phe] and the monomer.[20] This eventually enhanced the percentage conversion and hydrophilicity of [BMIM][Phe].

Sorption Kinetics

Figure 6 shows the adsorption kinetics of the five kinds of polymers for L-Phe. Fast adsorption of L-Phe by MIP1, MIP2, and MIP3 were observed within the initial 30 min; this was followed by a slow increase in the adsorbed amount until adsorption equilibrium. However, a relative slow adsorption of L-Phe for NIP1 and NIP2 were obtained during the whole adsorption process. This fact indicated that the molecular imprinting sites in the MIPs took an important role in the initial adsorption, and the imprinting recognition was fast. This may have been related to their characteristic surface morphologies. It is known that the surface properties of the MIPs and NIPs have much influence on their binding properties.[21] In general, the pore structure directly affects the rate of mass transfer. Therefore, the MIPs and NIPs were characterized by nitrogen adsorption experiments, and the obtained surface area and average pore diameter values for the MIPs and NIPs are summarized in Table III. The surface areas of the MIP and NIP were determined to be 21.8 (MIP1), 15.6 (MIP2), 10.7 (MIP3), 2.2 (NIP1), and 4.9 m^2/g (NIP2). The average pore diameters of the MIPs and NIPs were 23.4 (MIP1), 22.4 (MIP2), 20.7 (MIP3), 10.8 (NIP1), and 8.3 nm (NIP2). Thus, after the polydivinylbenzene beads were covered with imprinted copolymer, especially the polymer

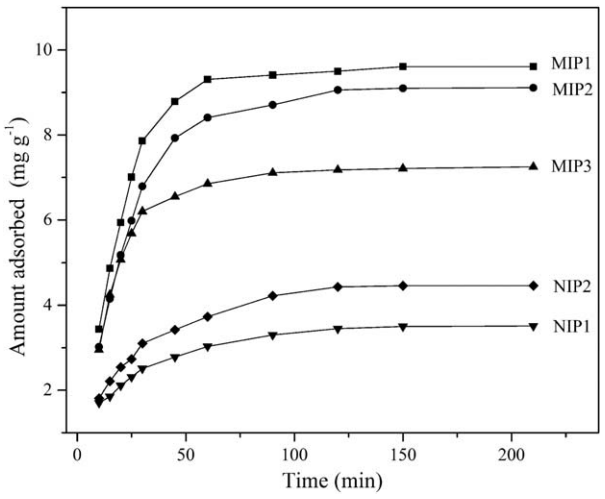

Figure 6. Adsorption kinetic curves for L-Phe (1.4 mg/mL) in deionized water: experimental data for (A) MIP1, (B) MIP2, (C) MIP3, (D) NIP2, and (E) NIP1.

Table III. Conversion Percentages of the Shells of the NIPs and MIPs and Surface Properties

Polymer	Conversion percentage (%)[a]	Surface area (m^2/g)	Pore diameter (nm)
MIP1	92.12	21.8	23.4
MIP2	96.33	15.6	22.4
MIP3	44.05	10.7	20.7
NIP1	45.21	2.2	10.8
NIP2	55.07	4.9	8.3

[a] The conversion percentages of the shells were calculated with the following equation:

$$\text{Conversion} = (m_{\text{core-shell}} - m_{\text{core}})/m_{\text{FM}} \times 100\%$$

where $m_{\text{core-shell}}$ is the mass of the core–shell MIPs or NIPs and m_{core} and m_{FM} are the feed masses of the core and functional monomers, respectively.

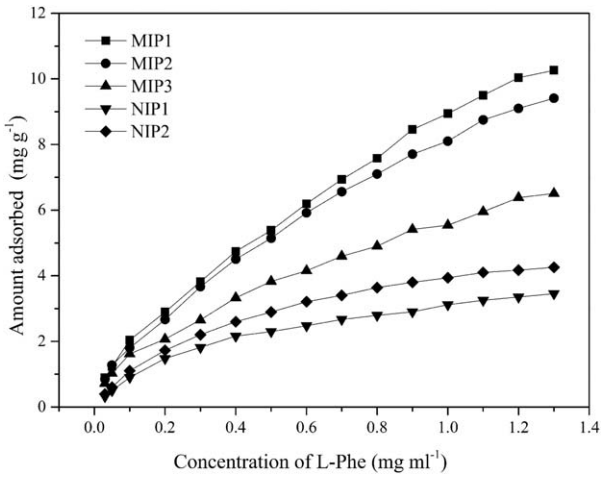

Figure 7. Adsorption isotherms of the polymers: (A) MIP1, (B) MIP2, (C) MIP3, (D) NIP2, and (E) NIP1.

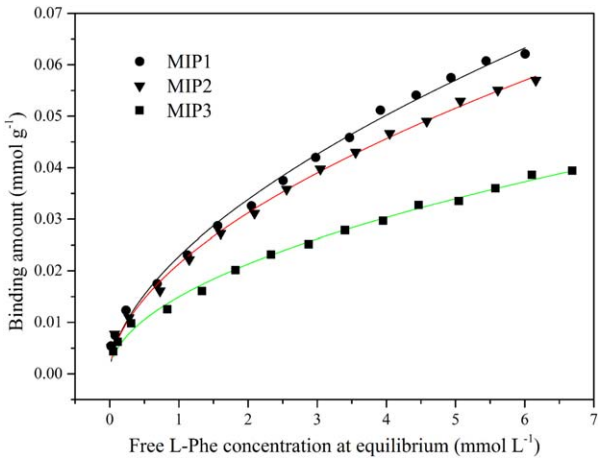

Figure 8. Adsorption isotherms of L-Phe on (A) MIP1, (B) MIP2, and (C) MIP3 nonlinearized according to the Freundlich equation. [Color figure can be viewed in the online issue, which is available at www.interscience.wiley.com.]

imprinted by [BMIM][Phe], they exhibited larger pores sizes distributed on the surface compared to those in the polymer imprinted by L-Phe in acetonitrile/H_2O. This eventually sped up the mass transfer rate and reduced the analysis time. Compared with the conventional method, the polymer imprinted by [BMIM][Phe] could be potentially applied more in real-time separation fields.

Sorption Isotherms and Molecular Recognition Mechanism of the MIPs

The adsorption isotherms of MIP1, MIP2, MIP3, NIP1, and NIP2 are illustrated in Figure 7. The adsorbed amount of L-Phe rapidly increased with increasing concentration of L-Phe in the initial stage; this was followed by a slow increase until adsorption equilibrium, and it reached saturation at a high L-Phe concentration. The maximum adsorption capacities of MIP1 and MIP2 were about 57.6 and 44.5% higher than that of MIP3, respectively. In general, the large surface area of the sorbent had a high adsorption capacity.[22] According to the nitrogen adsorption experiments, the surface area of MIP1 and MIP2 were larger; this was attributed to the solvent environment and the template. Water in the imprinting process was not the decided factor affecting the adsorption performance of MIPs, whereas the type of the template changed its adsorption properties significantly.

Isotherms of the Freundlich form have been observed for a wide range of heterogeneous surfaces, including activated carbon, silica, clays, metals, and polymers.[23–26] Generally noncovalent MIPs are characterized by a heterogeneous distribution of binding sites with different affinities and selectivities.[27] Therefore, the Freundlich sorption model may be more suitable to MIPs than others. To further investigate the adsorption mechanism of L-Phe onto the polymers, Freundlich isotherm analysis were carried out to estimate the binding properties:

$$B = aF^r \tag{3}$$

where B is the amount of L-Phe bound to MIPs at equilibrium (mmol/g), F (mmol/L) is the free analyte concentration at equilibrium, a is the pre-exponential factor, r is the heterogeneity index, and a is a measure of the binding capacity (N) and average affinity (K_0), where K_0 is the average affinity.[28] The value of r varies from 0 to 1. An increase in r represents a decrease in the heterogeneity. We obtained the values of r and a from the fitting results. However, FI could not provide sufficient information for the exact solution of its affinity distributions.[28] We calculated the corresponding affinity distributions of the MIPs with eq. (4):

$$N(K) = 2.303am\left(1 - m^2\right)e^{-2.303m}\log K \tag{4}$$

$$K_{\max} = \frac{1}{F_{\min}} \tag{5}$$

$$K_{\min} = \frac{1}{F_{\max}} \tag{6}$$

$F_{\min}$ and $F_{\max}$ was defined as the maximum free concentration of the analyte and the minimum free concentration of the

Table IV. Freundlich Isotherm Models Calculated for the MIPs

Sequence	a	r	R^2	F_{error}[a]
MIP1	0.0228 ± 0.0006	0.5694 ± 0.0198	0.9934	216
MIP2	0.0214 ± 0.0005	0.5473 ± 0.0162	0.9951	152
MIP3	0.0150 ± 0.0004	0.5090 ± 0.0152	0.9929	101

[a] $F_{error} = (n-2)\sum(B_{exp,i} - B_i)^2/(n-1)\sum(B_{exp,i} - B_{calc,i})^2$
where n is the number of experimental points, $B_{exp,i}$ is an experimental point, B_i is the average of the experimental data points, and $B_{calc,i}$ is the corresponding calculated value, F_{error} is the statistical error, the higher F_{error}, the higher correlation between the model and the experimental data.

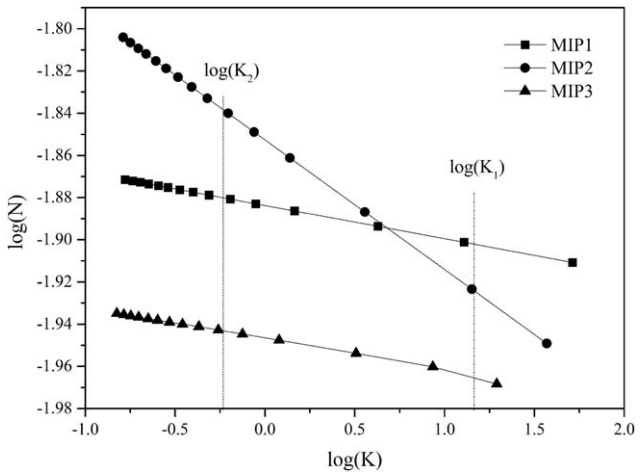

Figure 9. Affinity distributions of (A) MIP1, (B) MIP2, and (C) MIP3 based on the plotted Freundlich model. *N* and *K* are the binding capacity and the average affinity, respectively, K_1, K_2 are the high and the low value of affinity constant, respectively.

analyte ranges of the experimental binding isotherm, respectively. *K* is the affinity constant corresponding to different free concentration of the analyte of the experimental binding isotherm, where K_{max} and K_{min} are limited by the free concentration of L-Phe, K_{max}, K_{min} was the maximum and minimum values of *K* in the experiment, respectively [eq. (5) and (6)]. The Freundlich lines and fitting parameters are shown in Figure 8 and Table IV.

Compared with those in the literature,[29–31] the correlation coefficients (R^2) values were much higher; this indicated that adsorption of the prepared MIPs followed the Freundlich model. This may have been due to the multiple types of binding sites on the surfaces of MIP1, MIP2, and MIP3. The values of *m* suggested that the binding sites of the MIPs were heterogeneous. MIP1 showed the highest degree of binding site homogeneity with the highest heterogeneity index; these values were 4.0 and 14.4% higher than those of MIP2 and MIP3, respectively. Figure 9 shows the affinity distributions of L-Phe with MIP1, MIP2, and MIP3. At the high value of *K*, MIP1 and MIP2 have more high affinity binding sites than MIP3. This most likely arose from two sources. First, acetonitrile caused less damage to the template–monomer complexes than the organic–water binary solvent. Second, a higher affinity of 4-vp to [BMIM][Phe] in the polymerization process was more conducive to the realization of the adsorption of L-Phe from liquor. To summarize, the damage of water to hydrogen bonding caused the heterogeneity of binding sites and a smaller number of high affinity binding sites. The results indirectly illustrate that the MIPs imprinted by [BMIM][Phe] retained more specific binding sites because of stronger multiple interactions.

MISPE Analytical Application to Amino Acid Mixed Aqueous Solutions

To illustrate the potential of the MIPs for the recovery of L-Phe in the mixed sample, a comparison between the selected polymers were performed. The results are shown in Figure 10. MIP1, MIP2, and MIP3 were able to distinguish L-Phe from L-Trp and L-His, L-Phe was recognized by MIP1 with a recovery above 90.6%. However, the recoveries of the target molecule L-Phe were 82.0 and 71% for MIP2 and MIP3, respectively; this was significantly less than that of MIP1. L-Phe, L-Trp, and L-His were almost not discriminated on the NIPs. The recovery of MIP1 for L-Phe was 27.6% higher than MIP3. This was related to the following reasons: [BMIM][Phe] had stronger π–π and electrostatic interactions with 4-vp than L-Phe. More binding sites with a high affinity were created during the copolymerizing process in acetonitrile compared to the traditional imprinting process acetonitrile/H_2O. The advantage of binding sites homogeneous contributed the high selectivity of MIP1 on L-Phe according to the Freundlich analysis and the separation process.

Chiral Resolution of Racemic Phenylalanine

The changes in the CD spectra of different kinds of Phe solutions before and after adsorption are shown in Figure 11.

In aqueous solution, D-phenylalanine (D-Phe) contained a minimum negative CD absorption peak at 217 nm, and L-Phe had a positive CD peak at 217 nm, but its intensity was a little bit weaker than that of D-Phe. Therefore, the CD spectra of racemic phenylalanine showed a weak negative peak. To some extent, the CD spectral peak moved toward the direction of the D-Phe

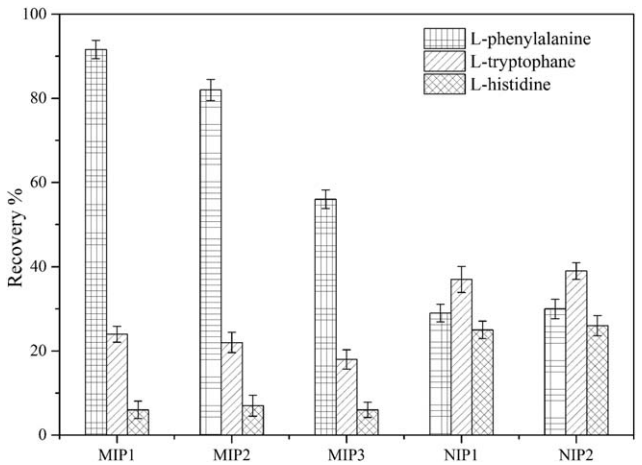

Figure 10. Comparison of the recovery performance of the MIPs.

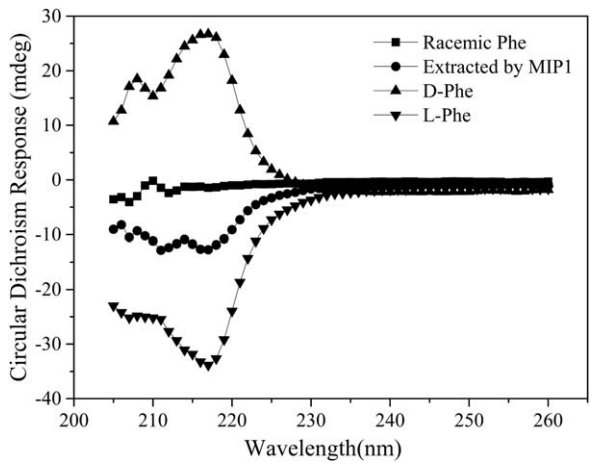

Figure 11. Chiral resolution of racemic phenylalanine by MIP1.

peak; this indicated that the MIP1 was selective for adsorbing the corresponding L-Phe molecules. This results manifest that the polymer imprinted by [BMIM][Phe] and ensured the integrity of the structure and conformation of L-Phe. As a result, we suggest that ionic interactions, hydrogen bonding along with π–π interaction between MIP1 and L-Phe, may have contributed to the resolution process. Further research is needed to investigate the imprinting mechanism of [BMIM][Phe] as a template.

CONCLUSIONS

In this study, oil-soluble AAILs were first applied to prepared surfaces of MIPs in acetonitrile for the selective recognition of L-Phe. The results show that the affinity of 4-vp to [BMIM][Phe] in acetonitrile was much higher than that of 4-vp to L-Phe. The results suggest that the recovery of MIP1 obtained were highest when the molar ratio of template to functional monomer and crosslinker was 1:6:24 compared with MIP3, which was prepared with a conventional template. Uniform MIP1 showed faster adsorption and much better selectivity for L-Phe than the traditional way made MIP3 from the adsorption dynamic studies and MISPE application. The Freundlich isotherm analysis demonstrated that the polymers imprinted by ILs in acetonitrile showed higher homogeneous binding sites than those prepared in the presence of water. An analysis of the CD spectra after the MISPE experiment for racemic phenylalanine solution showed that MIP1 also had the capability for specific chiral recognition for L-Phe to a certain extent. Accordingly, [BMIM][Phe] imprinting provided a new pathway for preparing amino acid MIPs in organic solvents.

ACKNOWLEDGMENTS

The financial support of the National Natural Science Foundation of China (contract grant numbers 21174111 and 51433008) is acknowledged.

REFERENCES

1. Hu, Y.-F.; Zhang, Z.-H.; Zhang, H.-B.; Luo, L.-J.; Yao, S.-Z. *Talanta* **2011**, *84*, 305.
2. Ilisz, I.; Aranyi, A.; Pataj, Z.; Péter, A. *J. Pharm. Biomed.* **2012**, *69*, 28.
3. Ma, Q.; Ma, M.; Tian, H.; Ye, X.; Xiao, H.; Chen, L.-H.; Lei, X. *Org. Lett.* **2012**, *14*, 5813.
4. Chen, Y.; Chen, L.; Bi, R.; Xu, L.; Liu, Y. *Anal. Chim. Acta* **2012**, *754*, 83.
5. Andersson, H. S.; Nicholls, I. A. *Bioorg. Chem.* **1997**, *25*, 203.
6. Blanco-López, M.; Lobo-Castanon, M.; Miranda-Ordieres, A.; Tunon-Blanco, P. *Trends Anal. Chem.* **2004**, *23*, 36.
7. Liang, R.; Zhang, R.; Qin, W. *Sens. Actuators B* **2009**, *141*, 544.
8. Asadi, E.; Azodi-Deilami, S.; Abdouss, M.; Kordestani, D.; Rahimi, A.; Asadi, S. *Kor. J. Chem. Eng.* **2014**, *31*, 1028.
9. Karlsson, J. G.; Andersson, L. I.; Nicholls, I. A. *Anal. Chim. Acta* **2001**, *435*, 57.
10. Urraca, J. L.; Hall, A. J.; Moreno-Bondi, M. C.; Sellergren, B. *Angew. Chem.* **2006**, *118*, 5282.
11. Nicolescu, T. V.; Sarbu, A.; Ovidiu Dima, S.; Nicolae, C.; Donescu, D. *J. Appl. Polym. Sci.* **2013**, *127*, 366.
12. Chen, L.; Xu, S.; Li, J. *Chem. Soc. Rev.* **2011**, *40*, 2922.
13. Alizadeh, T.; Zeynali, S. *Sens. Actuators B* **2008**, *129*, 412.
14. Tominaga, Y.; Kubo, T.; Kaya, K.; Hosoya, K. *Macromolecules* **2009**, *42*, 2911.
15. Fujita, K.; MacFarlane, D. R.; Forsyth, M. *Chem. Commun.* **2005**, 4804.
16. Mora-Pale, M.; Meli, L.; Doherty, T. V.; Linhardt, R. J.; Dordick, J. S. *Biotechnol. Bioeng.* **2011**, *108*, 1229.
17. Booker, K.; Bowyer, M. C.; Holdsworth, C. I.; McCluskey, A. *Chem. Commun.* **2006**, 1730.
18. Zhang, T.; Liu, F.; Li, K. *J. Appl. Polym. Sci.* **2013**, *129*, 3447.
19. Zhou, Y.; Tang, L.; Zeng, G.; Chen, J.; Cai, Y.; Zhang, Y.; Yang, G.; Liu, Y.; Zhang, C.; Tang, W. *Biosens. Bioelectron.* **2014**, *61*, 519.
20. Harrisson, S.; Mackenzie, S. R.; Haddleton, D. M. *Chem. Commun.* **2002**, 2850.
21. Pan, G.; Zu, B.; Guo, X.; Zhang, Y.; Li, C.; Zhang, H. *Polymer* **2009**, *5*, 2819.
22. Xie, S.; Svec, F.; Fréchet, J. M. *J. Chem. Mater.* **1998**, *10*, 4072.
23. Ng, C.; Losso, J. N.; Marshall, W. E.; Rao, R. M. *Bioresour. Technol.* **2002**, *85*, 131.
24. Umpleby, R. J.; Baxter, S. C.; Bode, M.; Berch, J. K.; Shaha, R. N.; Shimizu, K. D. *Anal. Chim. Acta* **2001**, *435*, 35.
25. Diñeiro, Y.; Menéndez, M. I.; Blanco-López, M. C.; Lobo-Castañón, J. M.; Miranda-Ordieres, A. J.; Tuñón-Blanco, P. *Biosens. Bioelectron.* **2006**, *22*, 364.
26. Cordoves, A. I. P.; Valdés, M. G.; Fernández, J. C. T.; Luis, G. P.; García-Calzón, J. A.; García, M. E. D. *Microporous Mesoporous Mater.* **2008**, *109*, 38.
27. Karlsson, B. C. G.; O'Mahony, J.; Karlsson, J. G.; Bengtsson, H.; Eriksson, L. A.; Nicholls, I. A. *J. Am. Chem. Soc.* **2009**, *131*, 13297.
28. Umpleby, R. J., II; Baxter, S. C.; Rampey, A. M.; Rushton, G. T.; Chen, Y.; Shimizu, K. D. *J. Chromatogr. B* **2004**, *804*, 141.
29. Allender, C. J.; Heard, C. M.; Brain, K. R. *Chirality* **1997**, *9*, 238.
30. Gao, B.; Guan, P.; Hu, X.; Qian, L.; Wang, Q.; Yang, L.; Wang, D. *Des. Monomers Polym.* **2015**, *18*, 185.
31. Fan, J. P.; Tian, Z. Y.; Tong, S.; Zhang, X. H.; Xie, Y. L.; Xu, R.; Qin, Y.; Li, L.; Zhu, J. H.; Ouyang, X. K. *Food Chem.* **2013**, *141*, 3578.